



Research Article

Assessment of a new rigid wall permeameter for the slurry like barrier materials: zeolite example

Gökhan ÇEVİKBİLEN*

Department of Civil Engineering, Istanbul Technical University, Istanbul and 34469, Türkiye

ARTICLE INFO

Article history

Received: July 12, 2023

Revised: September 01, 2023

Accepted: September 02, 2023

Keywords:

Zeolite, reactive barrier, permeability, effective stress

ABSTRACT

Areas vulnerable to catastrophic disasters such as hurricane, landslide and earthquake require ready and sustainable solutions for the post-pollution scenarios. Clinoptilolite type zeolite resources of Türkiye can serve economical and sustainable solutions as a quick response. While the studies on compacted zeolite-bentonite mixture at optimum water content for the landfill liners applications or dry zeolite-sand mixtures in permeable reactive barrier (PRB)s are common, the slurry form of zeolite emplacement at subsurface reactive barriers has not received an attention by the researchers. In this context, this experimental study presents the preliminary findings on one-dimensional consolidation and hydraulic conductivity tests performed on crushed zeolite samples S1 and S2 with fine contents of 33 and 84%, respectively. The results indicate that S2 has a higher compression index than S1, without a significant change in swelling index attributed to less than 4% clay contents. A self-designed rigid wall type permeameter was used to study on reconstituted slurry like materials under the benefit of back pressure saturation without the consolidation during testing that encountered in flexible wall permeameter. Falling head – rising tail water procedure was adopted under the back pressure in between 200 and 700 kN/m². S2 samples reconstituted under 25, 50, 100 and 200 kN/m² show a gradual decrease in k_v from 3×10^{-8} to 2×10^{-9} m/s. Previous observations on the sample of S1 revealed 8 times higher k_v values under the same σ_v' . Since the fine content of zeolite limits k_v , the proposed permeameter will be beneficial to determine the proper grain size distribution of fill materials considering the barrier height and in-situ stress conditions before the environmental studies with leachate.

Cite this article as: Çevikbilen, G. (2023). Assessment of a new rigid wall permeameter for the slurry like barrier materials: zeolite example. *J Sustain Const Mater Technol*, 8(3), 233–242.

1. INTRODUCTION

Hurricanes, landslides and earthquakes are one of the catastrophic disasters that result in economical and human losses globally. Decision makers are responsible to define and get precautions against this type of natural events that may affect their region locally. Since past, engineers have

been conducting scientific studies in geoenvironmental projects to reduce risk of loss of life and property. In this context, waste management strategies are discussed on sustainable solutions for post pollution events [1-7]. Based on the contamination scenarios, the barriers against the site-specific pollutants were previously studied considering

*Corresponding author.

*E-mail address: cevikbil@itu.edu.tr



the constructability, and readily available or near sources of the reactive fill material in the region for a quick and economical response.

Soil-bentonite (SB) and cement-bentonite (CB) based impermeable reactive walls are widely used to prevent the spread of contamination in the soil environment [8]. Fly ash [9] and steel slag [10] may also be used as ingredients that are effective to immobilize the contamination and increase the shear strength of the wall section. On the contrary, sand can be added to reduce the cost or increase the permeability of the barrier [11, 12] in case the permeable reactive barrier (PRB) methodology requires a more permeable material used in the barrier than the aquifer soil [8, 13-19] to control and treat the contaminated groundwater while passing through, based on its reactivity against the heavy metals [20, 21], chlorinated organics [22], radionuclides [23] etc in the soil. This alternative passive technology may involve one or more reactive materials in a barrier such as zero-valent iron (ZVI) [24-27], hydroxyapatite [28], and activated carbon [29] or natural rocks; limestone [30], attapulgite [31], sepiolite [32-34], zeolite [12, 33-36] which have been mechanically brought to a certain grain size or processed minerals such as organoclay [37-38] and organo-zeolite [38].

The constructability, stability and permeability of the wall section are reported to be related to the local geological and groundwater conditions [15, 39-41]. Emplacement methodology of a reactive material in an excavated trench defines the initial porosity along the barrier. However, it can be changed by inundation or in-situ stress conditions based on the initial moisture content (e.g. placement at dry state, a pre-designated water content, or in slurry form). In literature, there are limited number of studies about the stress distribution on the SB slurry trench cutoff walls [42-44]. The measured horizontal effective stresses within a 7 m high SB wall were pointed out to be considerably less than the expected geostatic stresses [43]. The hydraulic conductivity of SB is highly stress-dependent and increases with increasing fines content [43]. The stress dependency on hydraulic conductivity needs to be taken into consideration during design stage and this issue can be overcome by utilization of well graded backfill material [41]. However, it should be noted that these properties can change significantly when the fill material or construction methodology changes. Therefore, the environmental studies based on a single porosity value may not be sufficient to simulate the in-situ conditions of the reactive material especially when the barrier height increases, thus the porosity value decreases with increasing overburden stress. The performance of the barrier may be optimized by interpreting the porosity-overburden pressure-hydraulic conductivity relationship of a reactive material prepared at different grain size distributions. The breakthrough curves developed using the proper grain size of reactive material prepared at the designated porosity values will be beneficial to predict the longevity of the barrier.

Zeolite is one of the sustainable reactive materials applicable in remediation projects for groundwater pollution due to the high cation exchange capacity (CEC). [34-43]. Clinoptilolite-type zeolite showed more than 80% removal efficiency against the contaminants NH_4^+ , Pb^{+2} and Cu^{+2} ions in column and batch trials [12]. In that study, zeolite with a particle size range of 0.42–0.85 mm was amended with a local sand at a ratio of 20:80 (w/w) by mass to reduce the construction costs. Clinoptilolite-type washed zeolite had been found to be a suitable material for PRB considering the comparable shear strength of the mixture ($\phi=28.9^\circ$) with the aquifer soil ($\phi=27.3^\circ$), and higher permeability coefficient values of zeolite ($k=2 \times 10^{-5}$ m/s) than the aquifer soil ($k=7 \times 10^{-6}$ m/s). The field column tests were conducted to predict changes in the barrier during operation and to verify the longevity of barrier under the field conditions [12]. Villalobos et al. [45] performed compaction, consolidation and direct shear tests on compacted tuff zeolite with particle size of coarse sand, fine sand, silt and 15% clay reporting that the increase in fine fraction reduced the shear strength related to the higher water content which was attributed to the chemical structure of zeolite.

A significant portion of the world's zeolite reserves are in Türkiye [46, 47], thus there are a number of studies about the use of local zeolite in geoenvironmental practice [33-36, 48-51]. Tuncan et.al. [51] performed geotechnical tests on the compacted mixtures of bentonite, sand and fine size crushed natural zeolite and investigated the environmental characteristics when waste disposal leachate is used as an influent by analyzing Pb, Ni, Zn, Cu and Cr concentrations. The zeolite additive at 10% by weight was suggested for the landfill bentonite liners under municipal waste, which benefits from the high cation exchange capacity compared to the lean bentonite. Cevikbilen [35] compared the compression behavior of dry and inundated 67% sand, 33% fine particle size fraction of a local raw zeolite, and performed permeability tests to predict the hydraulic conductivity of a zeolite barrier along the depth of a trench by performing experimental and numerical analyses. The numerical models predicted that the hydraulic conductivity of the barrier would significantly decrease below 20 m depth considering the relationship observed experimentally between overburden pressure, void ratio and permeability. The shear strength of the inundated zeolite exhibits conservative values compared with the dry zeolite regarding to the result of the direct shear tests in which the shear strength angle ϕ decreased from 38 to 35° even though a slight increase of cohesion is observed.

Use of slurry form of the zeolite may be a proper emplacement methodology considering the observed values of high consolidation coefficients and the lower values of secondary compression and swelling indexes. Even though chemically identical composition and microscopic structure results in similar affinity towards pollutant removal from aqueous sources, the increase in the fine-grained fraction of zeolite may significantly reduce

the seepage velocity through a permeable barrier that may result in a scenario where the contaminated water bypasses the PRB. Hence, the effect of fine-grained fraction on the behavior of slurry-like zeolite should be discussed in advance to control the hydraulic conductivity along the barrier. In this respect, this study fills a gap about the effect of gradation on the permeability of a locally supplied raw Clinoptilolite-type zeolite rock prepared with mechanical crushers to be used as a reactive material at the sub-surface barrier. The hydraulic conductivity of zeolite emplaced in a trench at the slurry form was modelled experimentally after the consolidation stage under its self-weight using a rigid wall permeameter specifically designed for this study. Fine-grained zeolite was prepared at 1.5 times the liquid limit and applying one-dimensional compression allowed the consolidation of the samples under the overburden pressures within the range of 25 to 200 kN/m² to simulate the specimens in the deeper depths of the subsurface barrier with lower values of porosity. The permeability tests were conducted on these samples in the self-designed permeameter, which offered the advantage to apply a back pressure up to 700 kN/m² after the fully saturation had been verified. The comparison of void ratio - vertical effective pressure - the hydraulic conductivity relationship observed for the two specimens of crushed zeolite with different gradations presented that any increase in the fine particle size fraction or the overburden pressure decreased the hydraulic conductivity significantly. Consequently, an arrangement in grain size distribution of the same source reactive material from finer through coarser proportional with overburden pressure was proposed to improve the remediation performance along the depth of a subsurface barrier in harmony with the hydraulic conductivity of the adjacent soil profile.

2. MATERIALS AND METHODS

The source of the zeolite was from the Gördes district of Manisa province in Türkiye. Commercially available two fractions of the raw samples were supplied from the Gördes Zeolite Company. Fig. 1 shows the grain size distribution of samples S1 and S2 which have the particle sizes in between 0 - 2.0 mm, and 0 - 0.2 mm, respectively. The index properties of the samples were determined with respect to the relevant standards summarized in Table 1. Swelling potential of the zeolite was 3.5 mL/2g according to the ASTM D5890 method [52].

The zeolite specimens of the region are mostly reported to contain hydrated K, Ca, Mg, Na alumina-silicates [57]. Studies on identification and the origin, mineralogical and petrographic analysis of the rock samples of the source material with X-Ray Diffractometer illustrates that the major chemical compositions of the zeolite of this study are 71.6% SiO₂, 11.3% Al₂O₃, 3.67% K₂O, 2.27% CaO and the others are less than 1% by weight [35, 58]. Consequently, it is classified in 70~85 % Clinoptilolite-type zeolite group with the ratio of SiO₂/Al₂O₃ in between 5.0~6.3% at the source.

Table 1. Index properties of zeolite

Sample	S1	S2	Standard
Gravel (%) (>4.76 mm)	-	-	ASTM D6913 [53]
Sand (%) (4.76-0.075 mm)	67	16	ASTM D6913 [53]
Silt (%) (0.075-0.002 mm)	29	82	ASTM D7928 [54]
Clay (%) (<0.002 mm)	4	2	ASTM D7928 [54]
D ₈₅ (mm)	0.600	0.077	
D ₅₀ (mm)	0.164	0.030	
D ₁₅ (mm)	0.014	0.008	
D ₁₀ (mm)	0.0069	0.0055	
Liquid limit, LL (%)	58	55	ASTM D4318 [55]
Plastic limit, PL (%)	39	38	ASTM D4318 [55]
Plasticity index, PI (%)	19	17	ASTM D4318 [55]
Specific unit weight, G _s	2.39	2.38	ASTM D854 [56]

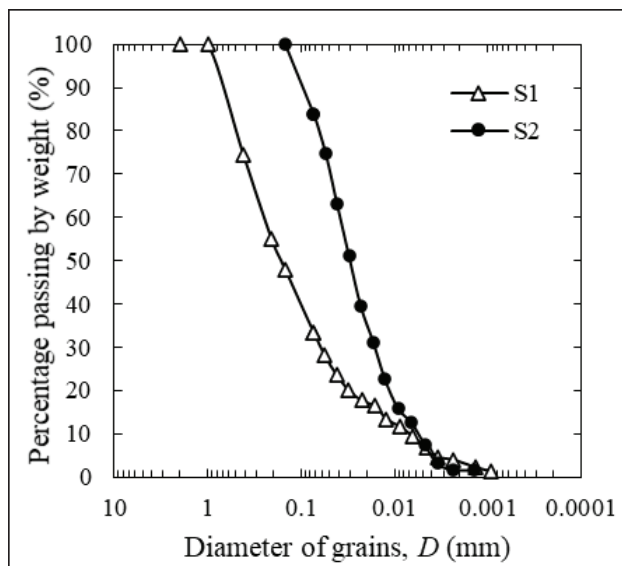


Figure 1. Grain size distribution of the samples.

Uygun et.al [57] compared the zeolites of two mining companies in Gördes region and presented that Gördes Zeolite Company had more impurities and involved tectosilicates such as 5% cristobalite and tridymite. The Scanning Electron Microscope (SEM) image taken at 3000 magnification factors of the zeolite sample used in the study (Fig. 2) confirms that the shape of the particles is varying from needle-shaped zeolite fibers to spherical-shaped amorphous structures.

The zeolite samples were prepared in the slurry form at water contents equal to 1.5 times the liquid limit. After the 24 hours of conditioning period of the slurry in a sealed container, a glass funnel was used while placing the remixed slurry samples in the test molds. Keeping the tip of the funnel inside the slurry, the tip was gradually raised from bottom to top. Thereafter, lateral light strokes were applied to the mold to minimize the air voids and finally a stainless-steel spatula was used to level the surface of the slurry.

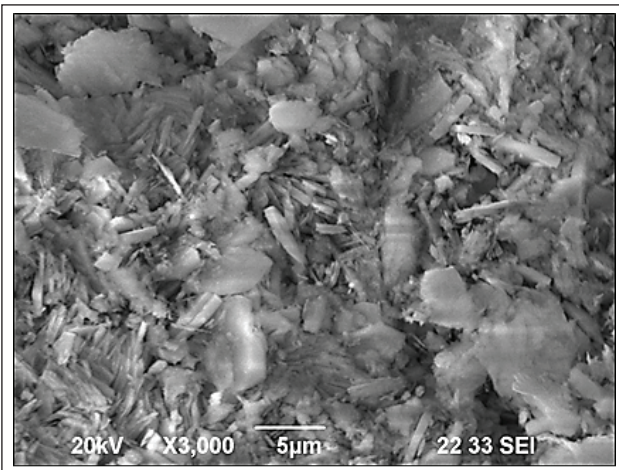


Figure 2. SEM image of Zeolite (x3000) [59].

One dimensional consolidation behavior of the samples was investigated in a consolidometer with an inner diameter of 63 mm and height of 40 mm. Two-way drainage was allowed at the top and bottom ends with the porous stones. The vertical loading was applied with a unit increment ratio in accordance with ASTM D2435 [60]. Time dependent vertical displacement were recorded by LVDT to check the end of primary consolidation at each load increment in a predesignated load duration of 24 hours.

Permeability tests of the zeolite samples were conducted in a new rigid wall stainless steel mold within the

45×45×45 mm inner dimensions. A front-loading arm type conventional consolidation test frame was modified to reconstitute the slurry at a predesignated overburden pressure in the mold on which an extension collar was initially attached. After a seating pressure of less than 5 kN/m² had been applied, the vertical load was gradually increased up to final effective consolidation pressure σ'_v values of 25, 50, 100 or 200 kN/m². During the reconstituting, a unit load increment ratio was adapted and the load increment durations were at least 24 hours. As in consolidometer, two-way drainage was allowed through the top and bottom porous ends. After the primary consolidation had finalized with respect to the settlement versus time data recordings, the cell chamber and the collar were removed. Then the excess height of each sample was trimmed, and the top cover of the mold was closed which has a porous end mounted inside. The vertical permeability test with respect to falling head – rising tail water procedure was performed with respect to Method C of ASTM D5084 [61] on the reconstituted samples in the mold which were connected to a Trautwein M100000 standard pressure panel through the top and bottom ends. Time dependent influent and effluent volumes of water passing through the sample was followed through the burettes on the panel during the test. The experiments were repeated at least 4 times under condition at which the hydraulic gradient was less than 5. Fig. 3 summarises the steps of the sample preparation and testing procedure.

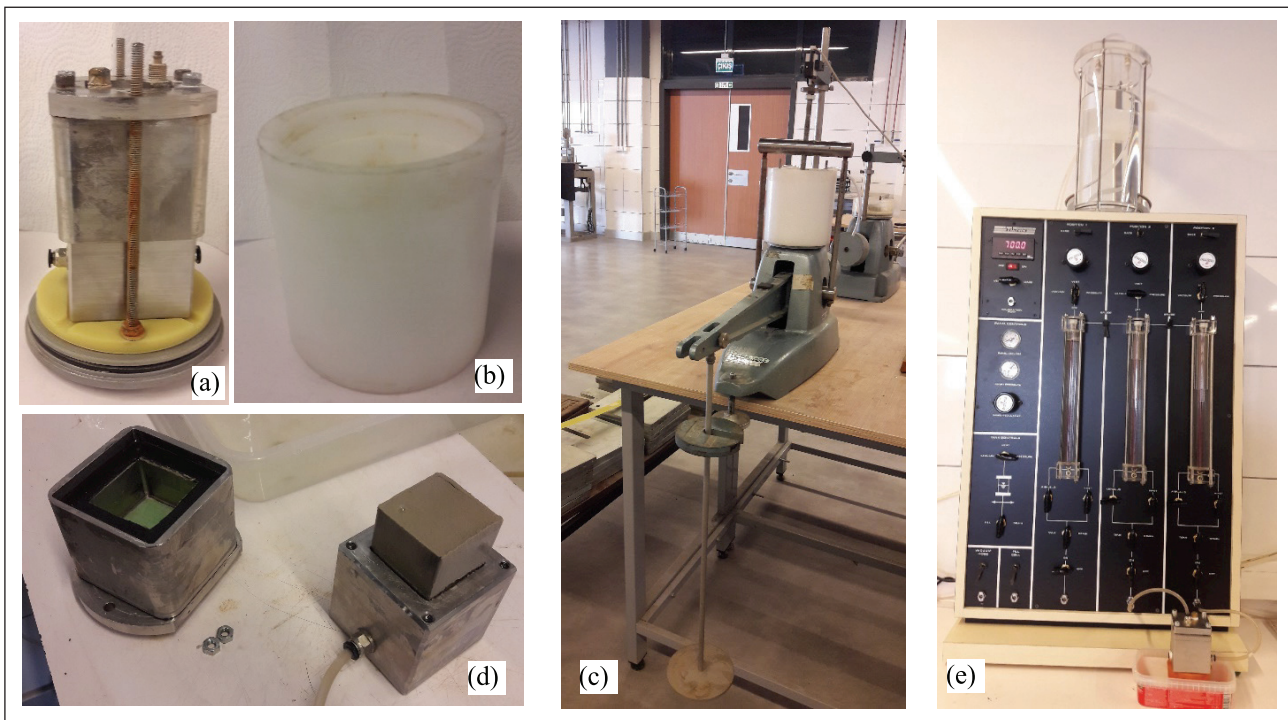


Figure 3. (a) Mold with collar piece (b) consolidation cell chamber (c) reconstituting S2 sample under 50 kN/m² consolidation pressure at modified front loading arm consolidation test setup (d) the sample before trimming after the collar piece was removed (e) the permeability test under 700 kN/m² back pressure.

3. RESULTS AND DISCUSSION

The subsurface barriers can be constructed as impermeable, permeable or the combination of both to limit, direct or treat the pollution in a contaminated region. While the k values of SB below 1×10^{-7} m/s are assumed to be sufficient for slurry cut off walls, in case of PRBs the k value of the reactive barrier should be higher than the aquifer soil. The fine content in fill material plays an important role on the hydraulic conductivity of the barriers. Since the construction methods and economic factors limits the installed thickness of the barriers less than 2 m in the direction of the groundwater flow for the zeolite-based barriers [14, 39], the use of proper graded samples in testing programs is essential. The sorption capacity and residence time inputs used in the mathematical models to predict the necessity in reactive material replacement will have a significantly impact on the economics of the system.

Before the long-term laboratory tests, the index properties of the fill material and the aquifer soil may be used for preliminary assessments to determine the interaction between them. Based on their grain size distribution, the filtration criteria stated by [62] as

$$D_{15 \text{ filter}} < 5 \times D_{85 \text{ soil}} \quad (1)$$

$$4 < \frac{D_{15 \text{ filter}}}{D_{15 \text{ soil}}} < 20 \quad (2)$$

$$D_{50 \text{ filter}} < 25 \times D_{50 \text{ soil}} \quad (3)$$

can be used to arrange the gradation of fill material considering the soil environment. Contrary, designating the soil type of the environment for a specific filler is applicable. In this context, the listed values in Table 1 presents that sample S1 will be a proper filter material for a soil stratum in which $D_{85} > 0.0028$ mm, $D_{50} > 0.0065$ mm, 0.0035 mm $> D_{15} > 0.0007$ mm. while sample S2 is proper for a soil with $D_{85} > 0.0016$ mm, $D_{50} > 0.0012$ mm, 0.0020 mm $> D_{15} > 0.0004$ mm. Hence, S2 offers a better filtration potential if the soil stratum has higher fine size particle content.

Since the zeolite in the slurry form at the initial case has direct contact with the aquifer soil, seepage property of zeolite can also be checked. The solid particles in the slurry, cannot permeate or can permeate the soil stratum or can flow out through the pores in soil stratum with respect to the n parameter $n < 2$ or $2 < n < 4$ or $n > 4$ respectively which is defined by

$$n = \frac{0.2 \times D_{15 \text{ soil}}}{D_{85 \text{ solid in slurry}}} \quad (4)$$

In case of a slurry composed of S1 and S2 samples, the zeolite particles cannot seep, can seep, or flow out through the pores in the soil stratum which has $D_{15} < 6$ mm, $6 \text{ mm} < D_{15} < 12$ mm or $D_{15} > 12$ mm, and $D_{15} < 0.77$ mm, $0.77 \text{ mm} < D_{15} < 1.54$ mm or $D_{15} > 1.54$ mm, respectively. Considering a homogenous aquifer soil condition, S1 has

lower seepage potential than S2 that S1 is properly used in sand and fine-grained soils, while S2 is applicable in only fine-grained soils.

The consistency limit tests presented that S1 has slightly higher value of liquid limit than S2 due to the higher amount of clay size particle. Practically, the change in fine fraction did not result in a significant change at plasticity and specific unit weight of the zeolite samples.

One dimensional consolidation behavior of the zeolite slurry samples S1 and S2, which have 33% and 84% fine fraction respectively, was determined. Fig 4 presents an example for the compression ratio versus logarithm of time plot observed under 100 kN/m^2 vertical pressure at S1. These recordings showed that primary consolidation duration is approximately 10 minutes for S1 under 100 kN/m^2 vertical stress. It was attributed to the predominant sand or silt size particles with the clay fraction below 4% for both of the samples. Therefore, it might be projected that zeolite-based barrier system in the field will settle under its own weight in a limited time domain which would consequently result in an apparent change in void volumes through the barrier with a direct impact on the performance of the barrier.

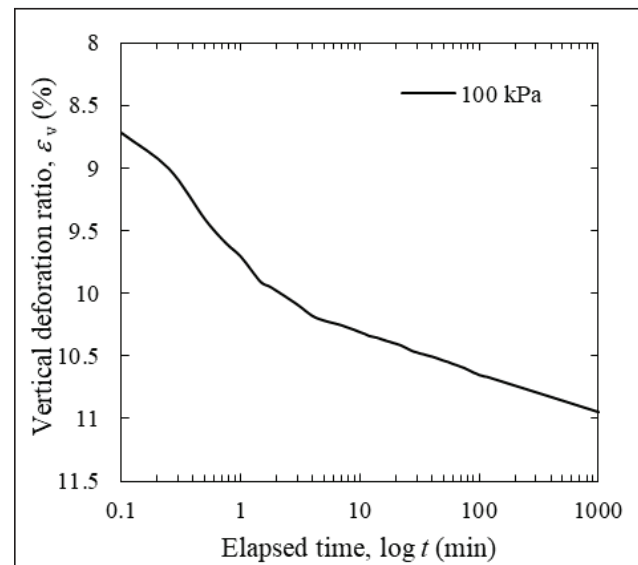


Figure 4. Consolidation behavior of S1 sample under 100 kN/m^2 stress level with time.

Consolidation curves of both S1 and S2 are presented in Figure 5. During loading stages, the void ratio values for S2 were observed higher than S1 at the same stress levels. However, at approximately 800 kN/m^2 , both consolidation curves converge to each other, indicating that the effect of fine fraction by weight was negligible. The compression index, C_c of S1 and S2 was calculated to be 0.225 and 0.264, respectively. Compression indices of Clinoptilolite type zeolite remolded at its liquid limit has been reported as 0.194, with an initial void ratio of 1.184, which is in

agreement with the results, since the initial void ratio of S2 is 1.47, hence a larger compression index is expected. For Terzaghi [63] proposed the compression index, C_c value for natural undisturbed soils as

$$C_c = 0.009 \times (LL - 10) \quad (5)$$

where LL : the liquid limit (in %). However, the predicted values around 0.400 by Equation 5 was lower than the observed values. In unloading stage performed after 800 kN/m², the swelling index, C_s of S1 and S2 was determined as 0.015 and 0.026, respectively in which S2 showed slightly higher values attributed to the higher fine content (Fig. 5).

The back pressure application is commonly used technique in triaxial testing to enhance the high degree of saturation of soil samples [64]. However, the saturation technique adopted in flexible wall testing cause an error considering the consolidation of the problematic soils sample due to the increase in effective stress under a constant total stress condition. Therefore, new permeameters were introduced such as low-compliance double cell/burette permeameter to track all volumetric changes during testing stages [65]. The rigid wall permeability cell proposed in this study is one of the permeameters that has the benefits of the back pressure application for the reliable characterization of saturated permeability and the constant void ratio of the reconstituted sample during testing. The vertical permeability tests were performed at several back pressure values. The higher back pressures present the faster saturation of the sample. Fig 6 shows the values of k_v versus back pressure observed in S2 sample under the back pressures in between 200 and 700 kN/m² when the hydraulic conductivity is steady.

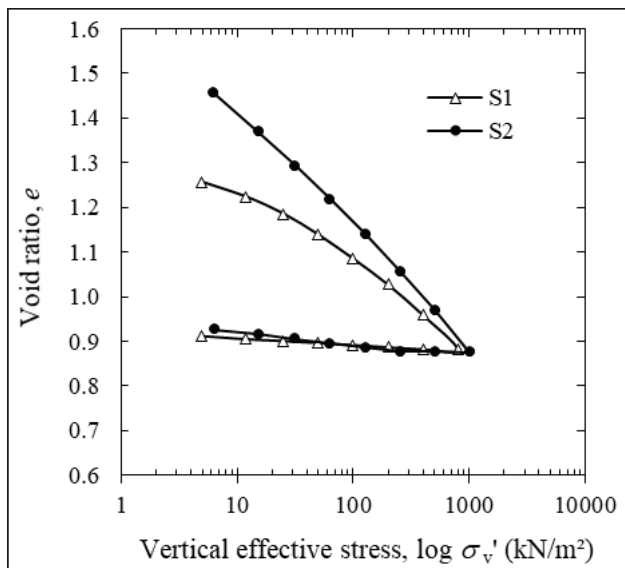


Figure 5. Consolidation behavior of the samples with vertical effective stress.

The ratio of inflow and outflow rate was controlled to be in the range of 0.75~1.25 as mentioned in ASTM D 5084 [60], which was slightly out of the limits at the back pressures below 400 kN/m² and in the range of 0.9~1.1 above 500 kN/m². So, the values of k_v observed at the back pressures above 500 kN/m² was assumed to be sufficient for fully saturation of the samples and taken into consideration which decreased slightly with back pressure.

Besides, the vertical permeability coefficient, k_v values versus back pressures did not change significantly, the average values of k_v observed above 500 kN/m² were used in this study. Fig. 7 illustrates k_v values of S2 samples reconstituted at 25, 50, 100 and 200 kN/m². The k_v - σ'_v relationship of the sample S1 in the previous study of Cevikbilen & Camtakan [34] is also plotted in Fig. 7. The permeability tests of that study were also performed under constant volume conditions in a ELE brand oedometer cell specialized to determine the vertical permeability. It was obvious that the k_v values were gradually decreased when σ'_v increased for both of the samples. Contrast to the values of e of the same source zeolite, the S2 sample with higher fine size particles revealed approximately 10 times lower values of k_v at the same σ'_v . The greater change in e values at higher fine fractions cause the greater reduction in k_v at the relevant σ'_v . On the contrary, the same values of k_v were determined at around 8 times lower σ'_v for S2 compared with S1. It is seen that the grain size distribution controls the hydraulic conductivity of crushed zeolite in slurry trench applications, which will affect the performance of the barrier. Ören and Özdamar [48] reported comparable hydraulic conductivity values for a compacted zeolite sample having a clay content of 3%.

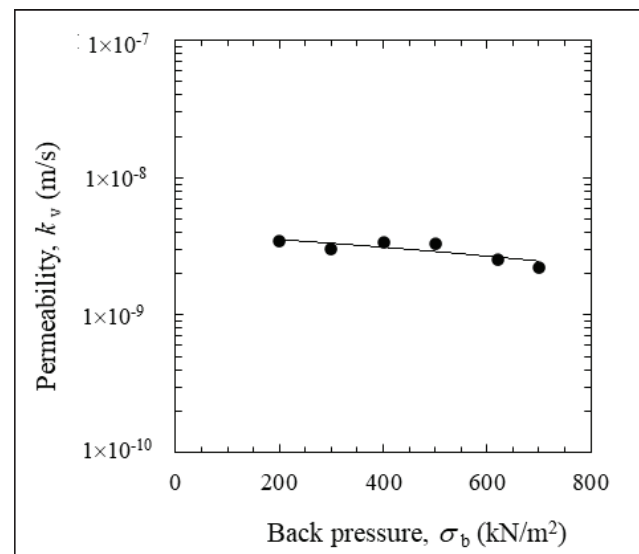


Figure 6. Permeability of S2 sample prepared at 200 kN/m² under several back pressures.

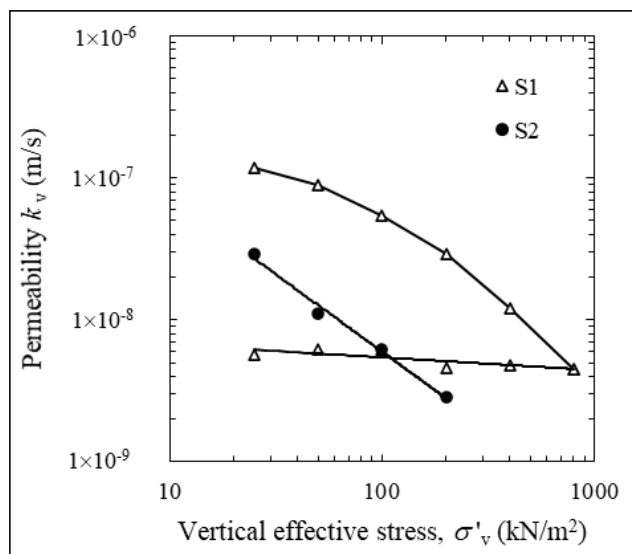


Figure 7. Permeability versus vertical effective stress for zeolite samples S1 and S2.

Hazen’s equation [66] for clean uniformly graded materials between permeability coefficient k (in m/s) was defined by

$$k = \frac{(D_{10})^2}{100} \quad (6)$$

where D_{10} : effective grain diameter (in mm) at which the soil weight. The predicted k values of S1 and S2 by Equation 6 are 4.7×10^{-7} and 3.0×10^{-7} m/s, respectively, which are higher than the observed values under any stress condition. So, environmental testing programs should involve the hydraulic conductivity tests on the final product at relevant overburden pressures for sustainable solutions.

In situ conditions, the reduction in effective overburden pressure along the barrier column is observed in the limited cases when the groundwater level rises or when an excavation is required. The low values of C_s for zeolite samples exhibit the swelling will be limited even though a slight increase was shown in Fig. 5 with an increase in fine fraction. Accordingly, unloading result no significant change in k_v for S1 sample despite the reduction in σ'_v from 800 to 25 kN/m² (Fig. 7). So, permeability tests at the unloading stage of S2 were not performed with respect to the low C_s value and the low swelling potential of the zeolite source material determined by ASTM D5890 [51].

4. CONCLUSION

The use of local reactive resources against environmental problems will reduce the application costs and enable quick response in case of a post-pollution scenario after a predictable disaster. The subsurface barriers offer sustainable solutions to limit, direct, immobilize or treat the site-specific pollutants that requires short- and long-term

laboratorial studies to predict the performance and longevity of the barrier before the construction. In this context a new rigid wall permeability cell was proposed for slurry like reactive materials that allow to study with the reconstituted samples under a vertical overburden pressure and eliminate the consolidation effect encountered during the flexible wall permeability tests. Following findings were obtained:

- The tests performed on S2 presented that k reduces with σ'_v which are below 10^{-7} m/s above 25 kN/m² overburden pressures and sufficient for impermeable wall sections. Further studies on thickening or dispersing agents will improve the flexibility, workability and sealing property of the slurry like fine grained zeolite for impermeable barrier applications.
- The comparison of the findings with the literature indicates that the higher k values are applicable by increasing the coarse particle size fraction of crushed zeolite. When the fine fraction in the slurry is reduced to 33%, k values are increased approximately 10 times than the zeolite with 84% fines under the same σ'_v conditions. Nevertheless, the use of slurry form of coarse-grained zeolite with 33% fines in PRB applications requires further investigation in which the k values are still lower than 10^{-7} m/s at σ'_v above 50 kN/m².
- This study further proposes hydraulic conductivity tests on the slurry like barrier material reconstituted at the relevant overburden pressures with respect to the height of the barrier to be involved in environmental testing programs.
- The new permeameter has promising advantages for the future works by helping to compose the porosity related breakthrough curves of a barrier material that may later be subjected to a site-specific leachate testing program for sustainable solutions.

ETHICS

There are no ethical issues with the publication of this manuscript.

CONFLICT OF INTEREST

The author declare that they have no conflict of interest.

DATA AVAILABILITY STATEMENT

The authors confirm that the data that supports the findings of this study are available within the article.

FUNDING

This research was financially supported by Istanbul Technical University Research Fund (ITÜ-BAP; project no MGA-43814) The author would like to thank the ITU, Faculty of Civil Engineering, Geotechnical Engineering Laboratories. The author appreciates Dr. Zeynep Camtakan for her help and support in this study.

REFERENCES

- [1] Kurihara, O., Tsuchida, T., Takahashi, G., Kang, G., & Murakami, H. (2018). Cesium-adsorption capacity and hydraulic conductivity of sealing geomaterial made with marine clay, bentonite, and zeolite. *Soils and Foundations*, 58,1173-1186. [CrossRef]
- [2] Vignola, R., Bagatina, R., D'Auris, A. F., Flego, C., Nalli, M., Ghisletti, D. et al. (2011). Zeolites in a permeable reactive barrier (PRB): One year of field experience in a refinery groundwater—Part 1: The performances. *Chemical Engineering Journal*, 178, 204–209. [CrossRef]
- [3] Puls, R. W., Blowes, D. W., & Gillham, R. W. (1999). Long-term performance monitoring for a permeable reactive barrier at the U.S. Coast Guard Support Center, Elizabeth City, North Carolina. *Journal of Hazardous Materials*, 68 (1–2), 109–124. [CrossRef]
- [4] DIPTAR. (2017). Deniz dip tarama uygulamalari ve tarama malzemesinin çevresel yönetimi final raporu, Project No: 111G036, TÜBITAK KAMAG 1007 Project, Kocaeli, Turkey. [Turkish].
- [5] Cevikbilen, G., Basar, H. M., Karadogan, Ü., Teymur B., Sönmez, D., & Tolun, L. (2020). Assessment of the use of dredged marine materials in sanitary landfills: A case study from the Marmara sea. *Waste Management* 113, 70-79. [CrossRef]
- [6] IAEA-TECDOC-1088 (1999). *Technical Options for the Remediation of Contaminated Groundwater*. International Atomic Energy Agency, Vienna, Austria. https://www.pub.iaea.org/MTCD/publications/PDF/te_1088_prn.pdf.
- [7] Nakayama, S., Kawase, K., Hardie, S., Yashio, S., Iijima, K., Mckinley, I., et al. (2015). *Remediation of contaminated areas in the aftermath of the accident at the Fukushima Daiichi Nuclear Power Station. Overview, analysis and lessons learned. part 1. A report on the "Decontamination Pilot Project"*. Japan Atomic Energy Agency. <https://jopss.jaea.go.jp/pdf-data/JAEA-Review-2014-051.pdf>.
- [8] Blowes, D. W., Ptacek, C. J., Benner, S. G., McRae, C. W. T., Bennett, T. A., & Puls, R. W. (2000). Treatment of inorganic contaminants using permeable reactive barriers. *Journal of Contaminant Hydrology*, 45(1), 123–137. [CrossRef]
- [9] Morar, D. L., Aydilek, A. H., Seagren, E. A., & Demirkan, M. M. (2011). leaching of metals from fly ash-amended permeable reactive barriers. *Journal of Environmental Engineering*, 138(8). [CrossRef]
- [10] Chen, R., Zhou, L., Wang, W., Cui, D., Hao, D., & Guo, J. (2022). Enhanced electrokinetic remediation of copper-contaminated soil by combining steel slag and a permeable reactive barrier. *Applied Sciences*, 12, Article 7981. [CrossRef]
- [11] Gueddouda, M.K., Lamara, M., Abou-bekr, N., & Taibi, S. (2010). Hydraulic behavior of dune sand-bentonite mixtures under confining stress. *Geomechanics and Engineering* 2(3), 213-227. [CrossRef]
- [12] Park, J. B., Lee, S. H., Lee, J. W., & Lee, C. Y., (2002). Lab scale experiments for permeable reactive barriers against contaminated groundwater with ammonium and heavy metals using clinoptilolite (01-29B). *Journal of Hazardous Materials*, 95(1–2), 65–79. [CrossRef]
- [13] Kacimov, A. R., Klammler, H., Il'yinskii, N., & Hatfield, K. (2011). Constructal design of permeable reactive barriers: groundwater-hydraulics criteria. *Journal of Engineering Mathematics*, 71(4), 319–338. [CrossRef]
- [14] Gavaskar, A. R. (1999), Design and construction techniques for permeable reactive barriers. *Journal of Hazardous Materials*, 68(1–2), 41-71. [CrossRef]
- [15] Gavaskar, A. R., Gupta, N., Sass, B., Janosy, R., & Hicks, J. (2000). Design guidance for application of permeable reactive barriers for groundwater remediation. Strategic Environment Research and Development Program, F08637-95-D-6004, Columbus, Ohio. p. 167. [CrossRef]
- [16] Obiri-Nyarko, F., Grajales-Mesa, S. J., & Malina, G. (2014). An overview of permeable reactive barriers for in situ sustainable groundwater remediation. *Chemosphere*, 111, 243–259. [CrossRef]
- [17] Bone, B. D. (2012). Review of UK guidance on permeable reactive barriers. *Taipei International Conference on Remediation and Management of Soil and Groundwater Contaminated Sites*, Taipei, Taiwan.
- [18] Interstate Technology & Regulatory Council Permeable Reactive Barriers Team (2005). *Permeable reactive barriers: Lessons learned/new directions. PRB-4*. Interstate Technology & Regulatory Council, Washington, D.C. <https://frtr.gov/pdf/prb-4.pdf>.
- [19] Scherer, M. M., Richter, S., Valentine, R. L., & Alvarez, P. J. J. (2000). Chemistry and microbiology of permeable reactive barriers for in situ groundwater clean up. *Critical Reviews in Microbiology*. 26(4), 221-264. [CrossRef]
- [20] Ludwig, R. D., McGregor, R. G., Blowes, D. W., Benner, S. G. & Mountjoy, K. (2005). A Permeable Reactive Barrier for Treatment of Heavy Metals. *Ground Water* 40(1), 59-66. [CrossRef]
- [21] Zhu, F., Tan, X., Zhao, W., Feng, L., He, S., Wei, L. et.al. (2022). Efficiency assessment of ZVI-based media as fillers in permeable reactive barrier for multiple heavy metal-contaminated groundwater remediation. *Journal of Hazardous Materials*, 424, Article 127605. [CrossRef]
- [22] Lai, K. C. K., Lo, I. M. C., Birkelund, V., & Kjeldsen, P. (2006). Field monitoring of a permeable reactive barrier for removal of chlorinated organics. *Journal of Environmental Engineering*, 132(2) 149-288. [CrossRef]

- [23] Simon, F. G., & Meggyes, T. (2015). Effective cleanup of groundwater contaminated with radionuclides using permeable reactive barriers. In: *Permeable reactive barrier, sustainable groundwater remediation*, CRC Press.
- [24] Cundy, A. B., Hopkinson, L., & Whitby, R. L. D. (2008). Use of iron-based technologies in contaminated land and groundwater remediation: A review. *Science of the Total Environment*, 400(1–3), 42–51. [CrossRef]
- [25] O'Hannesin, S. F., & Gillham, R. W. (1998). Long-term performance of an in situ "iron wall" for remediation of VOCs, *Ground Water*, 36(1), 164–170. [CrossRef]
- [26] Henderson, A. D., & Demond, A. H. (2007). Long-term performance of zero-valent iron permeable reactive barriers: a critical review. *Environmental Engineering Science* 24(4), 401-423. [CrossRef]
- [27] Korte, N. E. (2001). Zero-valent iron permeable reactive barriers: a review of performance. United States Environ. Sciences Division Pub. No. 5056, U.S. Department of Energy, Washington DC. [CrossRef]
- [28] Moore, R., Szecsody, J., Rigali, M., Vermuel, V., & Luellen, J. R. (2016). assessment of a hydroxyapatite permeable reactive barrier to remediate uranium at the Old Rifle Site, Colorado – 16193. *M2016 Conference*, March 6 – 10, Phoenix, Arizona, USA.
- [29] Xiaoa, J., Pangb, Z., Zhoua, S., Chua, L., Ronga, L., Liua, Y. et al. (2020). The mechanism of acid-washed zero-valent iron/activated carbon as permeable reactive barrier enhanced electrokinetic remediation of uranium contaminated soil. *Separation and Purification Technology*, 244, Article 116667. [CrossRef]
- [30] Sanchez, M. J. M., Sirvent, C. P., Lorenzo, M. L. G., Lopez, S. M., Espinosa, V. P., Ciudad, E. G. et al. (2017). Permeable reactive barriers for the remediation of groundwater in a mining area: results for a pilot-scale project. *Geophysical Research Abstracts*, EGU General Assembly, 19, EGU2017-9275-1.
- [31] Anang, E., Hong, L., Fan, X., & Asamoah, E. N. (2021). Attapulgite supported nanoscale zero-valent iron in wastewater treatment and groundwater remediation: synthesis, application, performance and limitation. *Environmental Technology Reviews*, 11(1), 1-17. [CrossRef]
- [32] Lago, A., Silva, B., & Tavares, T. (2021). Cleaner approach for atrazine removal using recycling bio-waste/waste in permeable barriers. *Recycling* 2021, 6(2), 41. [CrossRef]
- [33] Camtakan, Z. (2021). Investigation of the treatment of cesium in waste storage areas with the permeable reactive barrier (PRB) system. [Ph.D. Dissertation]. Ege University, Izmir.
- [34] Cevikbilen, G., & Camtakan, Z. (2020). *Benchmark studies of a permeable reactive barrier system for radiocesium removal*. EGU General Assembly, EGU2020-13162. https://presentations.copernicus.org/EGU2020/EGU2020-13162_presentation.pdf. [CrossRef]
- [35] Cevikbilen, G. (2022). An assessment of the mechanical behavior of zeolite tuff used in permeable reactive barriers. *Geomechanics and Engineering an International Journal*, 31(3), 305-318.
- [36] Erdem, E., Karapinar, N., & Donat, R. (2004). The removal of heavy metal cations by natural zeolites. *Journal of Colloid and Interface Science*, 280(2), 309–314. [CrossRef]
- [37] Di Emidio, G., Flores, R. D. V., Scipioni, C., Fratolocchi, E., & Bezuijen, A. (2015). Hydraulic and mechanical behaviour of cement-bentonite mixtures containing HYPER clay: impact of sulfate attack. *6th Int. Symp. on Deformation Characteristics of Geomaterials*, Buenos Aires, Argentina, November.
- [38] Bagherifam, S., Brown, T. C., Fellows, C. M., Naidu, R., & Komarneni, S. (2021). Highly efficient removal of antimonite (Sb (III)) from aqueous solutions by organoclay and organozeolite: Kinetics and isotherms. *Applied Clay Science*, 203, Article 106004. [CrossRef]
- [39] USEPA. (2002). Field applications of in-situ remediation technologies: Permeable reactive barriers. Office of Solid Waste and Emergency Response Technology Innovation Office, Washington, DC.
- [40] Zhao, Z., Jing, L., & Neretnieks, I. (2010). Evaluation of hydrodynamic dispersion parameters in fractured rocks. *Journal of Rock Mechanics and Geotechnical Engineering*, 2(3), 243–254. [CrossRef]
- [41] Naidu, R., & Birke, V. (2015). *Permeable reactive barrier: sustainable groundwater remediation*. CRC Press Taylor & Francis Group, Boca Raton, FL, USA.
- [42] Malusis, M. A., Evans, J. C., Jacob, R. W., Ruffing, D. G., Barlow, L. C., & Marchiori, A. M. (2002). Construction and monitoring of an instrumented soil-bentonite cutoff wall: field research case study. *Proceedings of the 29th Central Pennsylvania Geotechnical Conference*, Hershey, PA, January.
- [43] Evans, J. C., & Ruffing, D. (2019). Stresses in soil-bentonite slurry trench cutoff wall. *Geo-Congress 2019*, GSP 312, 177-184. [CrossRef]
- [44] Tong, S., Wei, L.L., Evans, J. C., Chen, Y. M., & Li, Y. C. (2022). Numerical analysis of consolidation behavior of soil-bentonite backfill in a full-scale slurry trench cutoff wall test. *Soils and Foundations*, 62, Article 101188. [CrossRef]
- [45] Villalobos, F. A., Leiva, E. A., Jerez, Ó., & Poblete, M. E. (2018). Experimental study of the fine particles effect on the shear strength of tuff zeolites. *Journal of Construction*, 17(1), 23–37. [CrossRef]
- [46] USGS (2023). *World reserves of natural zeolites U.S. Geological Survey, Mineral Commodity Summaries, January 2023*. US Government Publishing Office, Washington, DC, USA. <https://pubs.usgs.gov/periodicals/mcs2023/mcs2023-zeolites.pdf>.

- [47] MTA. (2021). *Zeolite resources in Turkey*; MTA, Ankara, Turkey. www.mta.gov.tr/v3.0/sayfalar/hizmetler/images/b_h/zeolit.jpg.
- [48] Ören A H., & Özdamar T. (2013). Hydraulic conductivity of compacted zeolites. *Waste Management & Research*, 31(6) 634–640. [CrossRef]
- [49] Aksoy Y.Y. (2010). Characterization of two natural zeolites for geotechnical and geoenvironmental applications. *Applied Clay Science*, 50(1), 130–136. [CrossRef]
- [50] Erdem, E., Karapinar, N., & Donat, R. (2004). The removal of heavy metal cations by natural zeolites. *Journal of Colloid and Interface Science*, 280(2), 309–314. [CrossRef]
- [51] Tuncan, A., Tuncan, M., Koyuncu, H., & Guney, Y. (2003). Use of natural zeolites as a landfill liner, waste management & research. *The Journal for a Sustainable Circular Economy*, 21(1), 54–61. [CrossRef]
- [52] ASTM D5890. (2019). *Standard test method for swell index of clay mineral component of geosynthetic clay liners*. ASTM Int., West Conshohocken, PA, USA.
- [53] ASTM D6913. (2017). *Standard test methods for particle-size distribution (gradation) of soils using sieve analysis*. ASTM Int., West Conshohocken, PA, USA.
- [54] ASTM D7928. (2021). *Standard test method for particle-size distribution (gradation) of fine-grained soils using the sedimentation (hydrometer) analysis*. ASTM Int., West Conshohocken, PA, USA.
- [55] ASTM D4318. (2017). *Standard test methods for liquid limit, plastic limit, and plasticity index of soils*. ASTM Int., West Conshohocken, PA, USA.
- [56] ASTM D854. (2014). *Standard test methods for specific gravity of soil solids by water pycnometer*. ASTM Int., West Conshohocken, PA, USA.
- [57] Uygur V., Şanlı-Çelik C., Sukusu E. (2019). The effect of particle sizes on ammonium adsorption kinetics and desorption by natural zeolites. *Int J Agric for Life Sci* 3(2): 371-377.
- [58] TDGZ (2023). *Technical Datasheet for Gördes Zeolite CAS No: 12173-10-3*. Zeo Products. https://zeoproducts.com/assets/catalogues/tech_data_sheet/en/clinoptilolite.pdf.
- [59] MGA-43814-R2. (2023). Geçirimli reaktif bariyer uygulamaları için yeni bir deney düzeneği ve tasarım yöntemi geliştirilmesi: 2. ara rapor, T.C. İstanbul Teknik Üniversitesi Bilimsel Araştırma Projeleri Koordinasyon Birimi, genel araştırma projesi, İstanbul, Türkiye. [Turkish].
- [60] ASTM D2435. (2020). *Standard test methods for one-dimensional consolidation properties of soils using incremental loading*. ASTM Int., West Conshohocken, PA, USA.
- [61] ASTM D5084. (2016). *Standard test methods for measurement of hydraulic conductivity of saturated porous materials using a flexible wall permeameter*. ASTM Int., West Conshohocken, PA, USA.
- [62] Lambe, T. W., & Whitman, R. V. (1969). *Soil mechanics*, J. Wiley & Sons, NY, 553.
- [63] Terzaghi, K., & Peck, R. (1967). *Soil mechanics in engineering practice*. 2nd Edition. John Wiley, New York.
- [64] N. Naghavi, M. H. El Naggar. (2019) Application of back pressure for saturation of soil samples in cyclic triaxial tests. The proceedings of XVI Pan American Conference on Soil Mechanics and Geotechnical Engineering in the XXI Century: Lessons learned and future challenges, 115-123.
- [65] Sadeghi H., & Panahi P. A. (2020) Saturated hydraulic conductivity of problematic soils measured by a newly developed low-compliance triaxial permeameter, *Engineering Geology* 278, Article 105827. [CrossRef]
- [66] Taylor, D. W. (1948). *Fundamentals of soil behavior*. Wiley, New York. [CrossRef]